

## Sb/GaAs(110) interface: A reevaluation

F. Schäffler,\* R. Ludeke, A. Taleb-Ibrahimi, G. Hughes,<sup>†</sup> and D. Rieger<sup>‡</sup>  
 IBM Thomas J. Watson Laboratory, P. O. Box 218, Yorktown Heights, New York 10598  
 (Received 9 December 1986; revised manuscript received 27 March 1987)

The influence of thermal annealing on Sb/GaAs(110) interfaces is studied *in situ* by high-resolution photoemission spectroscopy. A detailed line-shape analysis of the Sb 4*d* core-level spectra shows that Sb deposition at room temperature (RT) does not lead to perfectly ordered growth of the first monolayer (ML), as was assumed so far. Annealing at 330°C results in a highly ordered overlayer that is desorption limited to 1 ML. The degree of order affects the barrier height at the interface drastically: While RT deposition pins the Fermi level 0.6 eV above the valence-band maximum for *p*-type GaAs, we find a reduction in the band bending by a factor of 2 after annealing.

The Sb/GaAs(110) interface has attracted several experimental and theoretical groups because of the epitaxial growth mode of the first Sb layer. Extensive low-energy electron diffraction (LEED) profile analysis has shown that the first monolayer (ML) of Sb closely resembles the topmost layer of the relaxed GaAs(110) surface.<sup>1,2</sup> Epitaxial Sb growth is limited to the first ML, followed by three-dimensional (3D) cluster growth (Stranski-Krastanov growth). Thermal desorption experiments have revealed the stability of the first ML up to temperatures of  $\approx 550^\circ\text{C}$ , while Sb in excess of 1 ML desorbs already at  $\approx 250^\circ\text{C}$ .<sup>3</sup> The electronic structure of the ordered Sb ML on GaAs(110) has been calculated by two groups.<sup>4,5</sup> Both find filled Sb-derived states below the ( $\Gamma$ -point) valence-band maximum (VBM), while the empty states are located above the conduction-band minimum (CBM) in the results of Ref. 5, but slightly below the CBM in those of Ref. 4. The model calculations imply that a ML of Sb should not affect the flat-band condition at the surface of clean cleaved *p*-type GaAs, but might result in a small Schottky barrier on *n*-type GaAs. However, the few band-bending measurements published so far are in gross disagreement with respect to each other: Schottky barriers of  $\approx 0.6$  eV for both *n*- and *p*-type GaAs were derived from work function measurements,<sup>6</sup> while surface-photovoltage (SPV) experiments indicate that an initial barrier created by a submonolayer coverage of Sb on *n*-type GaAs is largely removed at a coverage of 1 ML and above.<sup>7</sup> Raman experiments confirm the former results, but show additional changes at the interface for coverages exceeding several ML.<sup>8</sup> Angle-resolved photoemission experiments (ARPES) on cleaved *n*-type GaAs surfaces covered with 1 ML of Sb seem to show good agreement in the surface band dispersion with theory, especially for the highest filled surface bands,<sup>9</sup> the top of which was shown to coincide with the VBM of bulk GaAs. This coincidence, however, appears questionable, as the authors did not determine independently the position of the Fermi level at the Sb/GaAs interface, but used an uncharacteristically low value of 0.8 eV relative to the VBM quoted in the literature for cleaved *n*-type GaAs (Ref. 1) to determine the position of the Sb surface band. A larger value, as is suggested by the SPV results, would shift the top of

the filled surface band into the intrinsic band gap and thus could account for a Schottky barrier on *p*-type GaAs.

The samples for the mentioned LEED and band-bending measurements were prepared at room temperature (RT), which was considered sufficient for the growth of an ordered Sb ML. Since Sb evaporates as an Sb<sub>4</sub> molecule that has to dissociate at the surface in order to form a single layer, RT deposition is suspected to leave some imperfections in the first layer, which most likely would escape detection in a LEED experiment. If such a local disorder were to be associated with band-gap states, a very small density of the order of  $\frac{1}{1000}$  of a ML ( $\approx 10^{12}$  cm<sup>-2</sup>) of charged centers would be sufficient to create a Schottky barrier at the interface.

For these reasons we performed high-resolution core-level studies on RT-deposited and annealed Sb/GaAs interfaces, which provide both a measure for the degree of perfection in the overlayer and precise information about the band bending at the interface. The former is achieved by a detailed line-shape analysis of the Sb 4*d* signal, while the band bending is derived from the energy shifts of the Ga 3*d* and As 3*d* bulk signals. The experiments were performed at the National Synchrotron Light Source (NSLS) at the Brookhaven National Laboratory, in New York; details of the experimental setup have been published elsewhere.<sup>10</sup> Photoemission spectra were taken in an angle-integrated mode under surface-sensitive conditions (electron escape depths  $\leq 5$  Å). The combined resolution of analyzer and monochromator was estimated to be  $\leq 200$  meV. Zn-doped (*p*-type) GaAs samples with a carrier concentration of  $7 \times 10^{17}$  cm<sup>-3</sup> were cleaved *in situ* and tested for flat-band condition. All samples used for further studies showed an initial deviation from a flat band of  $< 50$  meV, resulting in a starting value of the Fermi level  $70 \pm 5^0$  meV above the VBM, as calculated from the bulk doping of the samples. Sb was evaporated from a BN effusion cell at typical rates of 0.3 Å/min. Evaporation rates were calibrated by long-term evaporation onto a quartz microbalance at the position of the sample. 1 ML of Sb, defined as two atoms per GaAs surface unit cell ( $\equiv 8.85 \times 10^{14}$  cm<sup>-2</sup>), corresponds to an equivalent thickness of 2.7 Å. The Sb overlayers were grown at RT and could subsequently be annealed at tem-

peratures up to 330 °C. No changes were observed in the 1×1 LEED pattern upon annealing. The core-level spectra were decomposed by means of a least-squares fitting procedure.<sup>11</sup>

Figure 1 shows the changes in the Sb 4d spectra for various coverages before and after annealing at 330 °C. Dots represent the data after subtraction of a smooth background, while the dashed and dash-dotted lines show the decomposition into two spin-orbit-split components; the solid lines give the sum of the components. Two distinct components are readily discernible for the annealed overlayers; for the unannealed samples the asymmetry of the peaks nevertheless suggests that at least two components are present as well. For a two-component fit both a smaller energy splitting and a larger full width at half maximum (FWHM) are obtained compared to the annealed case. These features are indicative of inhomogeneities in the bonding environment for each component, a notion which is physically more reasonable than the assumption of more than two underlying components with a FWHM of the annealed case. The energy splitting and FWHM of the two Sb 4d components for an Sb coverage of 1 Å (≈0.4 ML) are plotted versus annealing temperature in Fig. 2. Figure 3 shows energy splitting and FWHM as a function of coverage, which was obtained by

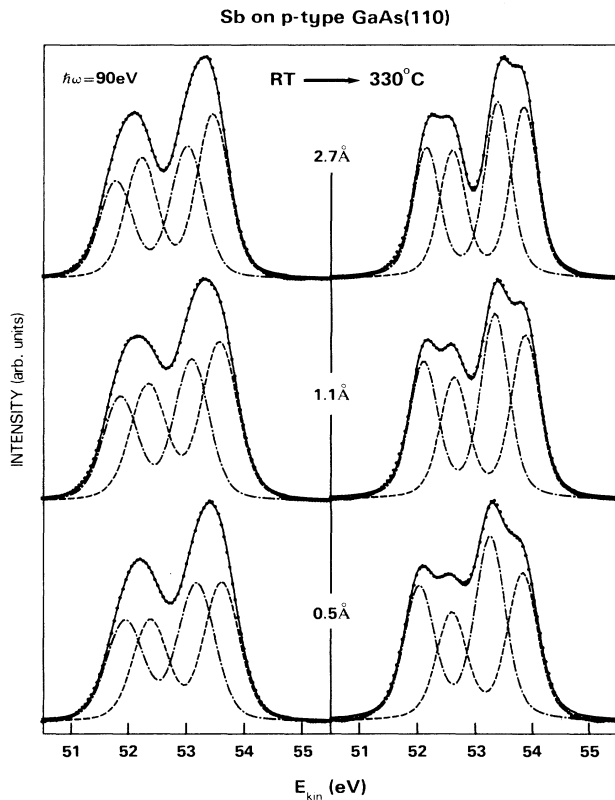


FIG. 1. Comparison between Sb 4d spectra of RT-deposited Sb overlayers and spectra of the same films after annealing at 330 °C. The dots represent the data and dashed lines and dash-dotted lines show the decomposition into the two components, which are summed up in the solid line. The highest coverage of 2.7 Å corresponds to 1 ML.

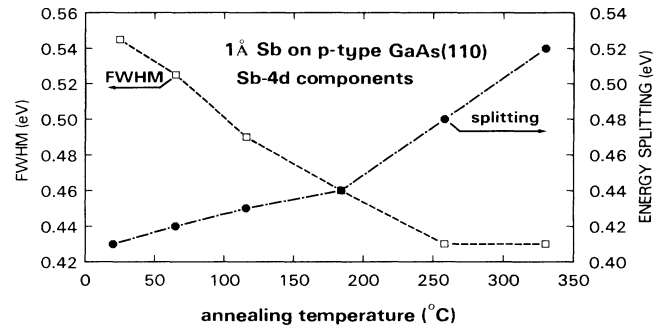


FIG. 2. Energy splitting and FWHM of the fitted Sb 4d components as a function of annealing temperature. The sample was covered with 1 Å of Sb at RT and annealed at increasing temperatures.

sequential RT deposition and annealing at 330 °C. This sequence leads not unexpectedly to slightly different values of the parameters at 1 Å as compared to the data in Fig. 2, which correspond to a single, uninterrupted deposition. Although the energy splitting between the two Sb core components does not appear to saturate at 330 °C—the highest “safe” annealing temperature in our experiments—we would not expect appreciable improvement in film quality beyond this value, as it is already sufficient to achieve the lowest FWHM, which is indicative of crystalline homogeneity.

The development of the Sb-4d signal as a function of temperature and coverage reveals several interesting features. (i) All spectra consist of two components. (ii) The FWHM of both components narrows with increasing annealing temperature concomitant with an increase in

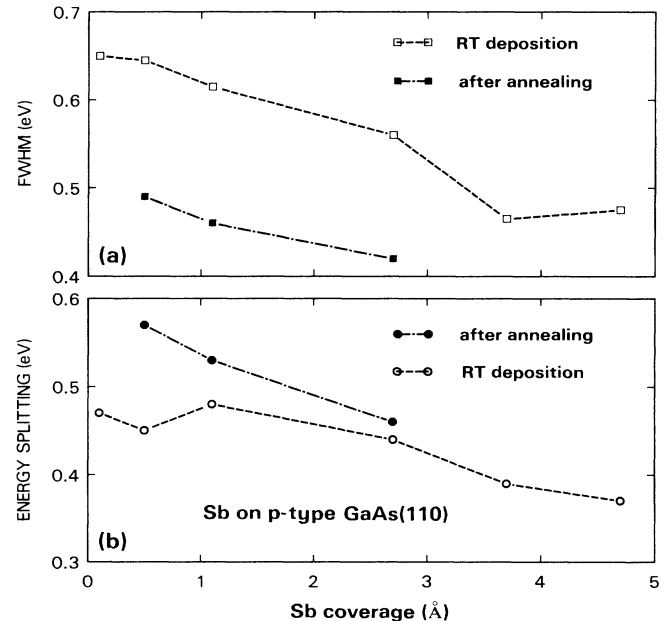


FIG. 3. (a) FWHM and (b) energy separation of the two Sb 4d components for RT-deposited Sb overlayers before and after annealing at 330 °C. The thickness of the annealed overlayers is desorption limited to 1 ML (2.7 Å).

their energy separation. An annealing temperature of 330 °C is necessary to achieve maximum resolution of the components (see Fig. 2). (iii) The high-kinetic-energy (KE) component of the RT-deposited Sb overlayers becomes larger with respect to the low-KE component for coverages above  $\approx 0.5 \text{ \AA}$  (see left panel in Fig. 1) and finally remains the only surviving component for a thick Sb overlayer (not shown). After annealing at 330 °C, the relation between the two components is reversed at lower coverages, but almost identical intensities are reached at 1 ML (see right-hand side of Fig. 1).

The temperature- and coverage-dependent line-shape analysis of the Sb 4*d* core level allows direct conclusions about the changes in interface morphology induced by annealing. The splitting into two components, which was also observed by Myron, Anderson, and Lapeyre,<sup>12</sup> results from the two different bonding sites in the first ML: According to the calculations<sup>4</sup> each Sb atom is covalently bonded to two Sb atoms along the zigzag chain and has a third bond to either a Ga or an As atom of the topmost GaAs layer. The Sb—As bond is covalent, while the Sb—Ga bond has partly ionic character, with charge accumulation around the Sb atom. This results in a shift of all electronic states related to the Ga site towards lower binding energies as compared to the states associated with the As site.<sup>4</sup> We therefore attribute the high-KE component in the Sb 4*d* spectra (which corresponds to lower binding energy) to Sb atoms with a Ga bond, the other one to the As sites. The perfect Sb ML is relaxed in a similar manner as the cleaved GaAs surface.<sup>2</sup> For GaAs the relaxation results in a shift of the Ga 3*d* and As 3*d* binding energies of the topmost layer in opposite directions.<sup>13</sup> We expect a similar behavior for the ordered Sb ML. Hence, the splitting in the two Sb 4*d* components should be largest for an ordered overlayer, while local nucleation on top of the first layer is expected to reduce the relaxation effect, resulting in a decrease of the splitting. Thus, we interpret the small splitting and the broadening of the components in the RT 4*d* spectra as evidence for random nucleation on top of first-layer Sb atoms already at submonolayer coverages. Thermal annealing, on the other hand, enhances the surface mobility of the Sb atoms, resulting in a reduction of 3D clusters and an increase of the ordered area. The highest annealing temperature studied (330 °C) lies above the desorption threshold for Sb atoms above the first ML and consequently suffices to remove all excess Sb. This argumentation is consistent with the changes observed in the intensity ratio of the components: Since the high-KE component finally merges into the single signal found for a thick Sb overlayer, its larger intensity at low coverages for the unannealed samples appears consistent with a premature 3D growth. After annealing, the low-KE component becomes larger, until equal intensity is reached at 1 ML. This is a consequence of the higher surface mobility, which enables Sb atoms to reach energetically favorable binding sites. As the ordered Sb layer gets much of its binding energy from the Sb—Sb bonds along the chains,<sup>4</sup> the preference of the As site is most likely limited to the end positions of chains with random length distribution. The termination of the Sb chains at As sites explains also the reduction in energy

splitting and FWHM with coverage as is observed for the annealed films (Fig. 3): The end atoms in each chain lack one Sb—Sb bond and hence have smaller volume charge surrounding them. The associated change in binding energy results in a larger component splitting and apparent broadening at low coverage, where the percentage of end atoms is largest. The absolute KE shifts of the two Sb components support this interpretation: We find that the change in energy splitting results from the low-KE component, while the other component follows the band bending within experimental error.

To study the influence of the overlayer morphology on the band bending at the interface, we measured the energy shift of the Ga 3*d* and As 3*d* core levels as a function of coverage for RT-deposited and annealed Sb overlayers. In either case we find no evidence for chemical shifts in these levels. Both core levels consist only of a bulk and a surface component. The latter disappears, as expected, once the surface is completely covered. Both bulk components show the same band-bending shift within experimental uncertainty ( $\leq \pm 40 \text{ meV}$ ). Figure 4(a) shows the Fermi-level shift with respect to the VBM for unannealed Sb overlayers on a *p*-type GaAs cleaved face. We observe a gradual increase in barrier height that reaches a value of 0.58 eV at 5 Å coverage. Although the variation of barrier height with coverage is in good agreement with the results of RT-deposited films reported in Refs. 6 and

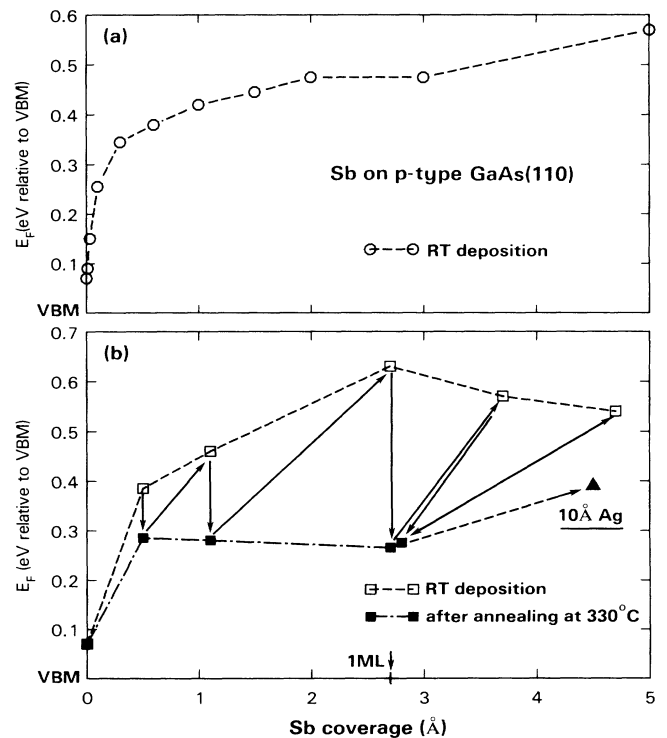


FIG. 4. Fermi-level shift relative to VBM for Sb-covered *p*-type GaAs cleaves. (a) Results for unannealed Sb overlayers on *p*-type GaAs cleaves. (b) Influence of annealing: Sb was evaporated at RT resulting in the band bending represented by open symbols. Subsequent annealing lead to a significant reduction in barrier height (full symbols). Arrows indicate the sequence of the experiment.

8, we found relatively poor reproducibility with variations of up to 200 meV for different cleaves. Annealing affects the band bending significantly, as is shown in Fig. 4(b): In this experiment Sb was deposited at RT in several steps, followed by annealing after each deposition. Photoemission spectra were recorded before and after annealing. We observe at all coverages a reduction in barrier height of up to a factor of 2. The barrier of the annealed sample is almost independent of overlayer thickness in the accessible coverage range, resulting in a final pinning position of the Fermi-level 280 meV above the VBM at 1 ML. RT evaporation of more Sb on an annealed, 1-ML-thick Sb film almost reestablishes the barrier height that was observed before annealing. This process is reversible, i.e., subsequent annealing (concomitant with thermal desorption, which reduces the integrated intensity of the Sb 4d signal to the value at 1 ML) results in the intrinsic barrier height of an ordered ML (see Fig. 4).

The Sb 4d core level studies and the band bending experiments allow the following conclusions.

(i) RT is not a suitable temperature to grow an ordered ML of Sb on GaAs(110). Films deposited at RT show local disorder and premature cluster growth on top of an incomplete first layer. This creates electronic states deep in the band gap, which pin the Fermi level  $\approx 0.6$  eV above VBM (*p*-type GaAs).

(ii) Annealing at temperatures above the desorption threshold for excess Sb leads to an ordered ML with a high degree of epitaxial perfection that reduces the pinning position to a value of 280 meV above the VBM. Valence-band photoemission experiments with the proper band-bending alignment show, under these conditions, Sb-derived emission in the band gap up to the Fermi-level.<sup>14</sup> This indicates that these states are largely responsible for the remaining barrier found on annealed samples. An accurate determination to within  $\pm 50$  meV of the top of the Sb surface band relative to the GaAs VBM can be obtained by detailed comparisons of the emission edges of the clean and Sb-covered samples, since they exhibit near-

ly identical emission onsets.<sup>4</sup> Our results indicate that after allowance for band bending, determined from the core level spectra, the maximum of the highest Sb surface band lies  $260 \pm 50$  meV above the bulk VBM of the GaAs. In contrast, theoretical predictions place the maximum at the VBM.<sup>4,5</sup>

(iii) Although annealing reduces the Schottky barrier on *p*-type and, most likely, also on *n*-type GaAs by about a factor of 2, an ordered ML of Sb does not passivate the GaAs surface, but rather behaves like the topmost layer of the clean (110) surface itself: Deposition of more Sb, which resembles the partly 3D morphology of the unannealed films, shifts the Fermi level several 100 meV higher into the band gap. We observe a similar behavior for Ag deposition onto an annealed Sb film, which results in a pinning position close to the one observed for an Ag-covered GaAs(110) surface (see Fig. 4).

The annealing experiments led to a consistent picture of the surface morphology of Sb overlayers on GaAs, which can explain most of the discrepancies in published results. However, the SPV measurements in Ref. 7 are hard to reconcile with our conclusions: Although the reported reduction in barrier height seems consistent with our results, we neither observe nor expect such a behavior upon RT deposition, and certainly not for coverages beyond 1 ML. It rather seems that SPV measurements, which actually measure work-function changes of the overlayer, are not a proper technique to study the band bending on the GaAs side of the interface. This conclusion is supported by the finding of semiconducting rather than metallic properties of up to 10-ML thick Sb overlayers on GaAs,<sup>8,15</sup> which make an interpretation of SPV experiments ambiguous.

We thank M. Prikas and the staff of the NSLS for their technical assistance. This work was supported in part by the U. S. Army Research Office under Contract No. DAAG-29-83-C-0026.

\*Present address: AEG, Fi22, Sedan Street 10, D-7900 Ulm, Federal Republic of Germany.

†Present address: School for Physical Sciences, National Institute for Higher Education, Glasevin, Dublin 9, Ireland.

‡Present address: Universität München, Sektion Physik, D-8000 München, Federal Republic of Germany.

<sup>1</sup>P. Skeath, C. Y. Su, I. Lindau, and W. E. Spicer, *J. Vac. Sci. Technol.* **17**, 874 (1980).

<sup>2</sup>C. B. Duke, A. Paton, and W. K. Ford, *Phys. Rev. B* **26**, 803 (1982).

<sup>3</sup>J. Carelli and A. Kahn, *Surf. Sci.* **116**, 380 (1982).

<sup>4</sup>C. M. Bertoni, C. Calandra, F. Manghi, and E. Molinari, *Phys. Rev. B* **27**, 1251 (1983).

<sup>5</sup>C. Mailhot, C. B. Duke, and D. J. Chadi, *Phys. Rev. Lett.* **53**, 2114 (1984); *Phys. Rev. B* **31**, 2213 (1985).

<sup>6</sup>M. Mattern-Klosson and H. Lüth, *Solid State Commun.* **56**, 1001 (1985).

<sup>7</sup>K. Li and A. Kahn, *J. Vac. Sci. Technol. A* **4**, 958 (1986).

<sup>8</sup>W. Pletschen, N. Esser, H. Münder, D. Zahn, J. Guerts, and W. Richter, in *Proceedings of the Eighth European Conference on Surface Science* [Surf. Sci. (to be published)].

<sup>9</sup>P. Martensson, G. V. Hansson, M. Lähdeniemi, K. O. Magnus-

son, S. Wiklund, and J. M. Nicholls, *Phys. Rev. B* **33**, 7399 (1986).

<sup>10</sup>D. E. Eastman, J. J. Donelon, N. C. Hien, and F. J. Himpsel, *Nucl. Instrum. Methods* **172**, 327 (1980); F. J. Himpsel, Y. Jugnet, D. E. Eastman, J. J. Donelon, D. Grimm, G. Landgren, A. Marx, J. F. Morar, C. Oden, R. A. Pollak, C. A. Schneir, and C. A. Crider, *Nucl. Instrum. Methods Phys. Res.* **222**, 107 (1984).

<sup>11</sup>G. Landgren, R. Ludeke, Y. Jugnet, J. F. Morar, and F. J. Himpsel, *J. Vac. Sci. Technol. B* **2**, 351 (1984); R. Ludeke and G. Landgren, *Phys. Rev. B* **33**, 5526 (1986).

<sup>12</sup>J. R. Myron, J. Anderson, and G. J. Lapeyre, in *Proceedings of the Seventeenth International Conference on the Physics of Semiconductors, San Francisco, 1984*, edited by D. J. Chadi and W. A. Harrison (Springer, New York, 1985).

<sup>13</sup>D. E. Eastman, T.-C. Chiang, P. Heimann, and F. J. Himpsel, *Phys. Rev. Lett.* **45**, 656 (1980).

<sup>14</sup>F. Schäffler, R. Ludeke, A. Taleb-Ibrahimi, and D. Rieger, *J. Vac. Sci. Technol. A* (to be published).

<sup>15</sup>M. Mattern-Klosson, R. Stümpler, and H. Lüth, *Phys. Rev. B* **33**, 2559 (1986).